



Florida Power

A Progress Energy Company

Crystal River Unit 3
Docket No. 50-302
Operating License No. DPR-72

Ref: 10 CFR 50.90

November 25, 2002
3F1102-11

U.S. Nuclear Regulatory Commission
Attn: Document Control Desk
Washington, DC 20555-0001

Subject: Crystal River Unit 3 – Submittal of Non-Proprietary Information Re: Proposed License Amendment Request #270, Revision 0, “Power Uprate to 2568 MWt” (TAC No. MB5289)

- References:
1. FPC to NRC letter, dated June 5, 2002, Crystal River Unit 3 – License Amendment Request #270, Revision 0, “Power Uprate to 2568 MWt”
 2. FPC to NRC letter, dated September 30, 2002, Crystal River Unit 3 – Response to Request for Additional Information Re: Proposed License Amendment Request #270, Revision 0, “Power Uprate to 2568 MWt” (TAC No. MB5289)

Dear Sir:

By letter dated June 5, 2002, Florida Power Corporation (FPC) submitted License Amendment Request #270, Revision 0, “Power Uprate to 2568 MWt.” In response to an NRC request for additional information dated September 30, 2002, FPC provided proprietary Framatome ANP document, FRA-ANP 51-5015662-01, “FIV Development, Qualification and Clarification for TMI”. The attachment to this letter provides the non-proprietary version of Framatome ANP document, FRA-ANP 51-5015662-01. Also being provided for NRC review is the non-proprietary version of Framatome ANP document, 86-5022636-00, “CR-3 PT Fluence Analysis Report – Cycles 7-10”.

This letter makes no new regulatory commitments.

If you have any questions regarding this submittal, please contact Mr. Sid Powell, Supervisor, Licensing and Regulatory Programs at (352) 563-4883.

Sincerely,

Dale E. Young
Vice President
Crystal River Nuclear Plant

DEY/pei

Attachments:

- A. Non-Proprietary Information - FRA-ANP 51-5015662-01, “FIV Development, Qualification and Clarification for TMI”
- B. Non-Proprietary Information - FRA-ANP 86-5022636-00, “CR-3 PT Fluence Analysis Report – Cycles 7-10”

xc: Regional Administrator, Region II
Senior Resident Inspector
NRR Project Manager

ADD

STATE OF FLORIDA

COUNTY OF CITRUS

Dale E. Young states that he is the Vice President, Crystal River Nuclear Plant for Progress Energy; that he is authorized on the part of said company to sign and file with the Nuclear Regulatory Commission the information attached hereto; and that all such statements made and matters set forth therein are true and correct to the best of his knowledge, information, and belief.


Dale E. Young
Vice President
Crystal River Nuclear Plant

The foregoing document was acknowledged before me this 25th day of November, 2002, by Dale E. Young.


Signature of Notary Public
State of Florida


(Print, type, or stamp Commissioned Name of Notary Public)

Personally Known X -OR- Produced Identification _____

FLORIDA POWER CORPORATION

CRYSTAL RIVER UNIT 3

DOCKET NUMBER 50 - 302 / LICENSE NUMBER DPR - 72

ATTACHMENT A

License Amendment Request #270, Revision 0, Power Uprate to 2568 MWt

**FRA-ANP 51-5015662-01, "FIV Development, Qualification and
Clarification for TMI"**

NON-PROPRIETARY



ENGINEERING INFORMATION RECORD

FRAMATOME ANP

Document Identifier 51 - 5022444 - 00

Title FIV Development, Qualification and Clarification for TMI
(Non-Proprietary Version of 51-5015662-01)

PREPARED BY:

REVIEWED BY:

Name JA Burgess JrName RR SchaeferSignature John A Burgess Jr. Date 11-19-02Signature RR Schaefer Date 11/20/02Technical Manager Statement: Initials JSB

Reviewer is Independent.

Remarks:

During a meeting with the NRC and TMI, a number of questions were presented with respect to the development of the Framatome ANP Flow Induced Vibration (FIV) methods for application to the OTSG. The historical, experimental, and analytical basis for the FIV methodologies is presented herein.

This document is the non-proprietary version of the proprietary document [51-5015662-01 or Reference 12]. In order for this document to meet the non-proprietary criteria, certain blocks of information were with-held based on the following criteria.

- a) Information reveals cost or price information, commercial strategies, production capabilities, or budget levels of FANP, its customers or suppliers.
- b) The information reveals data or material concerning FANP research or development plans or programs of present or potential competitive advantages to FANP.
- c) The use of the information by a competitor would decrease his expenditures, in time or resources, in designing, producing or marketing a similar product.
- d) The information consists of test data or other similar data concerning a process, method or component, the application of which results in a competitive advantage to FANP.
- e) The information reveals special aspects of a process method, component or the like, the exclusive use of which results in an advantage to FANP.
- f) The information contains ideas for which patent protection may be sought.



Record of Revisions

<u>Revision</u>	<u>Section</u>	<u>Description</u>	<u>Date</u>
00	All	Original Issue	11/2002

1.0 PURPOSE

The purpose of this document is to present the methodologies used to evaluate the Flow Induced Vibration (FIV) concerns of the OTSG tube bundle. This document will present both the techniques used to determine the OTSG secondary side thermal hydraulic conditions as well as their application to the structural FIV analysis. The qualification and accuracy of the thermal hydraulic and structural computer codes used in these evaluations are discussed. Lastly, recent test results of the cable stabilizer damping properties in regard to the fixed boundary conditions at the tubesheets and tube support plates, which result from an over-pressurized swollen tube, are presented.

2.0 BACKGROUND OF ORIGINAL OTSG TUBE FIV DESIGN CONSIDERATIONS

In the initial developmental stages of the OTSG design, which occurred during the late 1960's, Babcock & Wilcox performed numerous tests to assess the heat transfer characteristics and structural integrity of the OTSG shell and tube bundle. The mockup of the OTSG design was similar in length and other pertinent design considerations to that which was constructed for commercial operation with the exception of the number of tubes. The OTSG mockup was limited to 37 tubes. The OTSGs in service today have nearly 15,500 tubes.

The stability of the OTSG tube bundle was examined through qualitative test data and the experience on stability that were available when the design was first conceived. To provide the necessary confidence in the stability of the OTSG tube bundle, Babcock & Wilcox conducted an extensive research and development program to ensure that the OTSG tube would be fluid-elastically stable. The objectives of this program were to:

- (1) Determine experimentally the stability characteristics of the OTSG tube at design conditions;
- (2) Study experimentally the effect of various operating and physical parameters on the stability characteristics of the OTSG tube;
- (3) Develop an analytical tool by which the stability limits of the OTSG tube can be predicted.

A large amount of literature on the subject of fluid-elastic instability was reviewed and evaluated which provided an understanding of the phenomenon and led to an analysis code by which the stability limits of the OTSG tube bundle could be assessed. This code was also used to evaluate tube support plate configurations based on the instability ranges of the tube bundle. The capability of the analytical model used to evaluate the stability of the OTSG tube bundle was compared with the test results and other boiler designs currently in operation and found to predict the instability of a tube bundle with reasonable assurance.

Since the stability of the OTSG tube is directly related to the natural frequency of the tube, vibration testing was performed with a 0.625 inch OD Inconel tube 625.375 inches long, with a wall thickness of 0.035 inch. The tube was fixed at the ends to simulate the effect of the tubesheet and was supported between the ends by supports similar to those in the manufactured OTSG. The objective of testing performed with this mockup was to determine the possibility of buckling, vibration, and wear.

Vibration pluck testing of tubes on the actual fabricated commercial OTSG was performed in order to demonstrate that the production unit's vibratory response is in agreement with the sample tube test discussed above. The tubes tested in the production unit were found to have an average natural frequency of 47 Hz. This compared closely with the predicted value of 45 Hz.

The damping ratio was a second item considered in this program. In the single tube test, the average percent of critical damping was []^{b,d}. In the production unit test, the average percentage of damping was about []^{b,d}.

In conclusion, the pluck testing performed on the production unit demonstrated that the single tube laboratory testing as previously determined was representative of actual condition in the as-built OTSG units.

3.0 METHODOLOGIES FOR DETERMINATION OF THERMAL HYDRAULIC INPUTS FOR FIV ANALYSIS

Flow loads on OTSG tubes were originally based on tests on a scale model boiler described in Section 2.0. The velocity and density distributions in the top span were based on the following assumptions:

- The steam density is []^{b,d} lbm/ft³ and is uniform over the top span and over the entire cross section of the OTSG.
- The axial velocity distribution follows the []^{b,d} tubes. Thus, the actual cross flow velocity for each tube was []^{b,d}.

The secondary side mean velocity flow conditions, that were determined from testing, varied from tube-to-tube over the cross section of the OTSG. The maximum peak factor (ratio) from the mean velocity in each tube was []^{b,d} for the TMI OTSGs. The highest flow load occurred at []^{b,d}, at which the mean cross flow velocity was []^{b,d} ft/s. The highest predicted mean cross flow velocity for tubes []^{b,d} ft/sec.

Framatome ANP now uses a modified version of EPRI's "PORTHOS" computer code to predict detailed thermal-hydraulic performance of the OTSG. "PORTHOS" is a three-dimensional computational fluid dynamics computer code that models the tube bundle between the lower and upper tubesheet secondary faces. This modified version of "PORTHOS" has been adapted for OTSGs and its accuracy has been documented in Reference [7]. The OTSG thermal hydraulic model includes the aspirator port, tube support plates, peripheral gap between the tube support plates and the shroud, open tube inspection lane, and steam annulus. The current version does not include the feedwater downcomer, but does include the effects of steam-condensation heating of the feedwater. Applications of this code have included calculations of:

- (1) cross flow velocities and dynamic pressures in the upper span to support power uprates and definition of tube stabilization criteria,
- (2) moisture distributions in the upper span and at the upper tube sheet to establish localized and overall tube plugging limits, and

(3) mixed mean steam temperatures to support overall tube plugging limits.

The OTSG tubes are spaced on a triangular pitch. Thus, the tube orientation provides what appears to be a staggered alignment in some directions and an in-line alignment in others. The PORTHOS computer code models this effect using several parameters to account for the "porosity" of a steam generator tube bundle in its formulation. The volumetric porosity is used in the computation of cell pressures and the directional porosity values are used to compute gap velocities between the tubes. The directional porosity values are input for the axial, radial, and azimuthal directions.

It is believed that the hydraulic resistance of the tube bundle does not have a significant azimuthal dependence and the azimuthal variation in radial velocities is small. Thus, in PORTHOS modeling, the smaller of the two porosity values are input for both the radial and azimuthal porosity. This maximizes the velocities and is therefore, conservative. Framatome ANP is unaware of any test data that would confirm or refute this azimuthal variation of radial velocities.

The accuracy of the PORTHOS thermal hydraulic code and methods have been verified and thus its use in safety-related calculations is justified through favorable comparisons with model scale testing and plant data, References [9 through 11]. These comparisons include:

- Two different tests on 19 and 37 Tube Model Boiler tubes defining axial primary, tube, and secondary temperature distributions over the axial length as well as secondary pressure distributions
- Babcock-Atlantique Tube Bundle Cross Flow Velocity Distributions (with and without internal AFW headers)
- Plant Mixed Mean Steam Temperatures for 2568 Mwt nominal, 2772 Mwt nominal, 2568 Mwt with high peripheral plugging, and 2568 Mwt with three-tube wide inspection lane.

Many of these comparisons are presented in Reference [7] along with the comparison with plant mixed mean steam temperatures. Therefore, the use of PORTHOS to predict the OTSG secondary side conditions in the top span is justified for use as inputs into subsequent structural and FIV calculations.

Since PORTHOS lacked a turbulence model, corrections are made to accurately model the lower span of the OTSG. This short coming in PORTHOS limited the ability of the model to represent effects of fluid entrainment by the flow of streams jetting through the downcomer orifice which would be required to accurately predict the formation of any recirculation eddies.

Modifications to the PORTHOS coding have been made for the purpose of adding capability to model the orifice plate openings, lower downcomer, and baffle ports in the inlet region of the OTSG. PORTHOS models of the Chalk River (See Section 5.0) and ARC SG model configurations have been made and results compared with test data. PORTHOS results for velocity distributions over the SG inlet region at the tube bundle outer radius are considered reasonable. A conservative method is used to extrapolate velocity distributions at the outer radius to other radial locations within the lower bundle.

4.0 FIV ANALYSIS METHODOLOGIES

The general guidelines and methods employed by Framatome ANP for FIV analysis of heat exchanger tube banks are given in References [2 through 4]. For a virgin tube model, a single tube is modeled using finite element techniques provided by the Framatome ANP computer code "CASS". The tube is fixed at the secondary faces of the upper and lower tubesheet and pinned at all tube support plate locations. The effective mass of the tube, including the primary and secondary fluid, is considered in the modal analysis.

Once the frequencies and mode shapes of the tube have been determined, the Fluid-elastic Stability Margin (FSM) of the tube is evaluated with the Framatome ANP computer code "PCSTAB2". When a tube bundle is subjected to cross-flow with increasing velocity, it will come to a point at which the responses of the tubes suddenly increase without bound, until tube-to-tube impacting or other non-linear effects limit the tube motions. This phenomenon is known as fluid-elastic instability. The "PCSTAB2" computer code determines the margin against this instability of the tube from inputs such as;

- The mode shape eigenvalues from the modal analysis,
- Connors' constant,
- Damping values,
- Cross flow gap velocities,
- The linear mass densities of the tube, including non-structural and added masses
- Secondary side densities.

The computed Fluid-elastic Stability Margin (FSM) is the ratio of the critical velocity of the tube bundle (or the velocity at which the tube bundle is predicted to become unstable) to the equivalent mode shape weighted pitch velocity. An FSM greater than 1.0 implies that the tube is stable while and FSM less than 1.0 implies that the tube bundle is unstable. The minimum acceptable FSM for design is 1.0.

The stress from random vibration of turbulent cross flow is determined with the Framatome ANP computer code "PCRANDWIN". These vibrations are small in amplitude and always occur below the critical velocity and away from the vortex lock-in region. These small amplitude vibrations always exist and are caused by the turbulent eddies in the flow. The "PCRANDWIN" computer code determines these stresses using the coherence integral method and from inputs such as;

- The dynamic pressure ($\frac{1}{2}\rho V^2$),
- Damping ratio due to small vibration,
- A table to introduce the frequency dependence of the random lift coefficient and the correlation lengths

The vibration amplitudes due to vortex shedding are only computed for tubes located at the periphery of the bundle, as it is believed that the required vortices will not develop intra bundle. This response is also determined with the Framatome ANP computer code "PCRANDWIN". When vortex lock-in does occur, the forcing function becomes fully correlated over the span of the tube. Thus, vortex-induced vibration is determined by assigning a very large correlation length to the tube spans. The inputs for this analysis are similar to those provided for the turbulent buffeting vibration.

5.0 VERIFICATION OF FIV METHODOLOGIES

The Chalk River Nuclear Laboratory performed a stability test on a full scale model that consisted of the lower three spans of the B&W 177 Fuel Assembly OTSG. The actual span lengths, support plate thickness and tube-to-tube support plate clearances were properly simulated in this test. Results of these tests show that the tube bundle []^{b,d} lb/sec [Reference 5].

An analytical model of the Chalk River test tube was created to evaluate the FIV techniques and methodologies performed by Framatome ANP [Reference 6]. The analytical models predicted an FSM of []^{b,d} when using a Connors' constant of []^{b,d}, an axial damping value of []^{b,d} and a perpendicular damping value of []^{b,d} for the test above. Therefore, the overall analytical model predicted the instability threshold to within approximately []^b.

Framatome ANP has consistently used a Connors' constant of []^{b,d} for single phase flows in the bottom and top spans. An axial damping value of []^{b,d} and a perpendicular value of []^{b,d} are employed in the FIV analysis of OTSG tubes. The []^{b,d} axial damping is used to account for the frictional losses occurring between the tube and tube support plates as the tube slides vertically through the support plate. The contradiction in the constants employed in Framatome ANP FIV analysis and those determined from the Chalk River test can be in part eradicated through the relation of damping and the Connors' constant. The Fluid-elastic Stability Margin of a tube is proportional to the following parameters;

$$\beta\sqrt{\xi} = []^{b,d}$$

The combination of these two input parameters is believed to be realistic and not overly conservative by industry experts in the field of FIV. It closely corresponds to the Connors' constant of []^{b,d} and damping of []^{b,d} assumed in the calculation to correlate with the Chalk River test results. When $\beta = []^{b,d}$ and $\xi = []^{b,d}$ inputs are used, the fluid-elastic stability margin predicted for the Chalk River test setup is []^{b,d}; that is, with an accuracy of about []^{b,d}.

The uncertainties in calculating the FSM come from;

- (1) uncertainty in the fluid-dynamic input;
- (2) uncertainty in the damping ratio;
- (3) uncertainty in the stability constant.

Framatome ANP addresses (1) by using two different sets of input from two different sources, including the input from the "PORTHOS" computational fluid dynamics code and the older estimates that were actually extrapolated from a scale model test at the time the OTSGs were being designed. When all other input parameters are the same, the FSM values computed with these two different sets of fluid dynamic inputs are comparable, with the "PORTHOS" input giving results that are believed to be more accurate due to its more detailed modeling capability. Items (2) and (3) are addressed together by using a conservative estimate of damping ratio of []^{b,d} for loosely supported multi-span tube together with a conservative value for the stability constant []^{b,d}.

A test conducted at Babcock Atlantique over 25 years ago showed that the stability constant for the OTSG tube bundle was about [] while most of the industry data show stability constants over []. An in-air test of the full size OTSG conducted 25 years ago showed that even with moderate vibration amplitude well below the half tube-tube gap clearance, damping ratios mostly exceed []. Recent test in the lab using a one span beam with real OTSG support showed a damping ratio close to [] even for vibration amplitudes in the 0.01 inch range. Therefore, Framatome ANP believes the computed FSM for the OTSG tube is within [] accuracy.

Finally, we compare the final result with field experience. No OTSG tube in the designed condition has ever failed because of fluid-elastic instability. The latest incident regarding the severed tube at TMI verifies the technique. When testing was performed on an OTSG tube expanded against the support plate, the damping ratio significantly decreased. With this reduced damping ratio as input, the analysis showed that indeed tube 66-130 would be at the threshold of instability.

6.0 FIV DAMPING VALUES

Recent testing of the OTSG cable stabilizer to determine the additional damping the cable provides to the tube/cable system is presented in Reference [8] and summarized in Table 6.1. This testing was performed to determine the additional damping produced by the OTSG cable stabilizer in an over pressurized tube where the tube becomes locked into the tubesheets and tube support plates due to swelling of the tube. Several configurations are tested and the results for each system are summarized below.

Framatome ANP has traditionally used [] normal structural damping associated with non-linearity of the tube to TSP clearance. The test results shown in Table 6.1 show that the non-linearity of the tube to TSP clearance provides about [] damping. About [] of this damping is lost as a result of a swelled tube. When the tube pressurized, approximately [] additional damping is created. Since a pressurized tube would tend to restrain the tube more, it was concluded [] additional damping. This trend was also prevalent in the virgin tube and stabilized tube tests.

The viscous damping effect of secondary side fluids surrounding the tube that are in single phase is small, especially at temperatures of 550F, and is not typically considered in FIV analysis. However, 2% additional damping can be accounted for in the lower spans of the OTSG tube bundle where the secondary side fluid is in the two-phase mixture region.



Table 6.1: OTSG Cable Stabilizer Damping Results [Reference 8]

Test Case	Swelled Tube (yes/no)	Pressure (ksi)	Environment (air/water)	Stabilizer (yes/no)	TS Sever (yes/no)	Support Arrangement	% Damping (avg)
Baseline	no	0.0	air	no	no	(TS-TS) ⌈	⌈
1	no	0.0	air	no	no	(TS-D-B-TS)	
2	yes	0.0	air	no	no	(TS-D-B-TS)	
3	yes	0.0	air	yes	yes	(TS-D-B-TS)	
4	no	0.0	air	no	no	(TS-B-B-TS)	
5	yes	0.0	air	no	no	(TS-B-B-TS)	
6	yes	0.0	air	yes	no	(TS-B-B-TS)	
7	yes	0.0	air	yes	yes	(Sever-B-B-TS)	
8	no	0.0	air	no	no	(TS-B-B-B)	b,d
9	no	0.0	water	no	no	(TS-B-B-B)	
10	yes	8.0	water	no	no	(TS-B-B-B)	
11	yes	5.0	water	no	no	(TS-B-B-B)	
12	yes	0.0	water	no	no	(TS-B-B-B)	
13	yes	0.0	air	yes	no	(TS-B-B-B)	
14	yes	0.0	water	yes	no	(TS-B-B-B)	
15	yes	8.0	water	yes	no	(TS-B-B-B)	
16	yes	0.0	air	yes	yes	(Sever-B-B-B) ⌋	⌋

Notes: TS – Tubesheet Bore
D – Drilled Hole
B – Broached Hole

Summary of Damping Results:

Damping of tube (Fixed-Fixed) = ⌈ ⌈

Average damping of virgin tube in air =

Average damping of virgin tube in water =

Average damping of expanded tube w/o Pressure =

Average damping of expanded tube w/ Pressure = b,d

Average damping of expanded tube & stabilizer w/o Pressure =

Average damping of expanded tube & stabilizer w/ Pressure =

Average damping of swelled tube & stabilizer, with sever at TS, w/o Pressure = ⌋ ⌋

7.0 REFERENCES

- 1) [b,d], "Once-Through Steam Generator Research and Development Report", dated April 1971.
- 2) Ben Brenneman "Random Vibrations Due to Small-Scale Turbulence With Coherence Integral Method", ASME Journal of Vibration, Acoustic, Stress, and Reliability in Design, Volume 109, April 1987.
- 3) M. K. Au-Yang, "Flow-Induced Vibrations of Power and Process Plant Components," ASME Press, 2001. Chapters 7 and 9.
- 4) ASME Section III, Appendix N-1300 Series Non-mandatory Code on FIV Analysis of Tube Banks, 1998 Edition.
- 5) Once-Through Steam Generator (OTSG) Fluid-elastic Instability Study [b,d]
- 6) [b,d], "Flow-Induced Vibration Analysis of TMI OTSG Tubes due to Power Uprate", dated June 1997.
- 7) Moore, R.W. "Adaptation of PORTHOS to the Once-Through Steam Generator", Presented at an American Power Conference.
- 8) [b,d], "OTSG Cable Stabilizer Damping Test Results", dated November 2001.
- 9) [b,d], "PORTHOS for OTSG Application", dated January 1996.
- 10) [b,d], "OTSG Top Span Conditions – PORTHOS", dated April 1996.
- 11) [b,d], "OTSG Local Tube Plugging Limits", dated November 1998.
- 12) [b,d], "FIV Development, Qualification and Clarification for TMI", dated 12/2001.

FLORIDA POWER CORPORATION

CRYSTAL RIVER UNIT 3

DOCKET NUMBER 50 - 302 / LICENSE NUMBER DPR - 72

ATTACHMENT B

License Amendment Request #270, Revision 0, Power Uprate to 2568 MWt

**Non-Proprietary Information - FRA-ANP 86-5022636-00, "CR-3 PT Fluence
Analysis Report – Cycles 7-10"**

NON-PROPRIETARY

A

FRAMATOME ANP

CALCULATION SUMMARY SHEET (CSS)

Document Identifier 86-5022636-00Title CR-3 PT FLUENCE ANALYSIS REPORT - CYCLES 7-10

PREPARED BY:

REVIEWED BY:

METHOD: DETAILED CHECK INDEPENDENT CALCULATIONNAME JAMES W. NEWMAN, JR.NAME J. N. BYARDSIGNATURE *James W. Newman, Jr.*SIGNATURE *John N. Byard*TITLE ENGINEER IIIDATE 11/22/02TITLE ENGINEER IIDATE 11/22/02COST CENTER 41016REF. PAGE(S) 12-13TM STATEMENT:
REVIEWER INDEPENDENCEN/A for EG

PURPOSE AND SUMMARY OF RESULTS:

This document summarizes the results from the CR-3 PT Fluence Analysis for cycles 7-10. Fast Fluence Values for 15, 32, and 48 EFPY were computed for the following locations:

- Pressure Vessel Inside Surface Maximum Location
- WF-8 and WF-18 Longitudinal Welds (upper shell)
- SA-1580 Longitudinal Weld (lower shell)
- SA-1769 Circumferential Weld (max location)
- WF-70 Circumferential Weld (max location)
- Lower Plate Maximum Location
- Upper Plate Maximum Location

THE FOLLOWING COMPUTER CODES HAVE BEEN USED IN THIS DOCUMENT:

CODE/VERSION/REV

CODE/VERSION/REV

N/ATHE DOCUMENT CONTAINS ASSUMPTIONS THAT
MUST BE VERIFIED PRIOR TO USE ON SAFETY-
RELATED WORK

YES



NO

Record of Revision

Revision Number

Description

00

Original Issue

Table of Contents

1.0 Introduction.....4

2.0 Fluence Results5

3.0 Dosimetry Activity10

4.0 References.....12

Appendix A – Methodology14

1.0 INTRODUCTION

Over the last fifteen years, Framatome ANP (FANP) has developed a calculational based fluence analysis methodology,¹ that can be used to accurately predict the fast neutron fluence in the reactor vessel using surveillance capsule dosimetry or cavity dosimetry (or both) to verify the fluence predictions. This methodology was developed through a full-scale benchmark experiment that was performed at the Davis-Besse Unit 1 reactor,¹ and the methodology is described in detail in Appendix A. The results of the benchmark experiment demonstrated that the accuracy of a fluence analysis that employs the FANP methodology would be unbiased and have a precision well within the U.S Nuclear Regulatory Guide 1.190 limit of 20%.^{1,2}

The FANP methodology was used to calculate the neutron fluence exposure for cycles 7-8, cycle 9 and cycle 10 of the Crystal River 3 nuclear reactor. The methodology was also used to estimate fluences on the inner surface of the reactor vessel, as well as at specified weld locations on the vessel surface. The fast neutron fluence ($E > 1$ MeV) at each location was calculated in accordance with the requirements of U.S. Nuclear Regulatory Guide 1.190.²

The energy-dependent flux on the cycle 9 and cycle 10 capsules was used to determine the calculated activity of each dosimeter. Neutron transport calculations in two-dimensional geometry were used to obtain energy dependent flux distributions throughout the core. Reactor conditions were representative of an average over the cycle 7-8 irradiation period. Cycles 9 and 10 were treated individually, since there was a dosimeter capsule for each cycle. Geometric detail was selected to explicitly represent the dosimeter holder and the reactor vessel. A more detailed discussion of the calculational procedure is given in Appendix A. The calculated activities were adjusted for known biases (photofission, short-half-life, U-235 impurity, and non-saturation), and compared to measured activities directly. It is noted that these measurements are not used in any way to determine the magnitude of the flux or the fluence. The measurements are

used only to show that the calculational results are reasonable, and to show that the results for the CR-3 dosimeters are consistent with the FANP benchmark database of uncertainties.

2.0 FLUENCE RESULTS

Three irradiation periods were analyzed as part of the CR-3 PT fluence analysis, one for cycles 7-8, one for cycle 9, and one for cycle 10. Cycles 7 and 8 operated for a total irradiation period of 1033.8 EFPD, cycle 9 for 557.2 EFPD, and cycle 10 for 592.8 EFPD.

The incident fast fluence ($E > 1.0$ MeV) was calculated on the inner surface of the reactor vessel. The layout of the reactor vessel is shown in Figure 2-1.

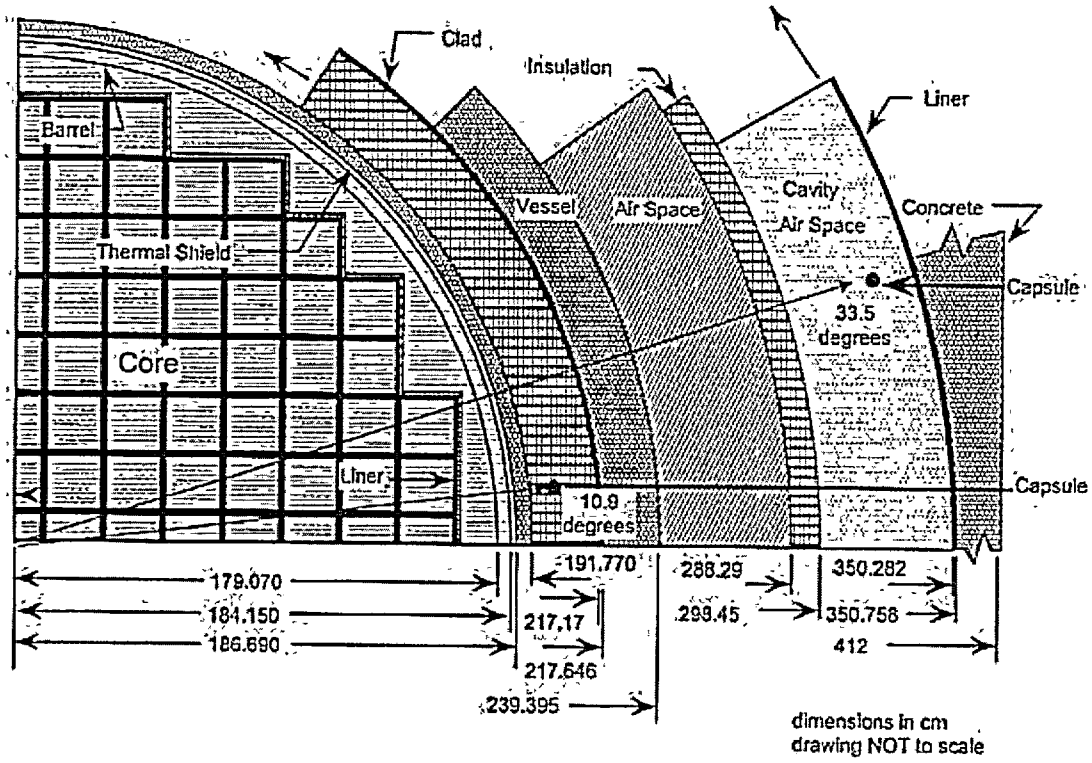


Figure 2-1. CR-3 Geometry Overview

Flux estimates were made for several points on the inner surface of the reactor vessel. These estimates are of particular importance in determining the effect of neutron fluence on the properties of the vessel surface and welds. The points of interest, and the calculated flux by cycle, are shown in Table 2-1.

Table 2-1. 3D Synthesized Fluxes

Cycle Length (EFPD)	Cycles 7 and 8	Cycle 9	Cycle 10
(EFPS)	8.9320E7	4.8142E7	5.1218E7
Flux Location	$E > 1.0$ MeV Flux (n/cm ² /s)		
Inside Surface Max. Flux	6.173E9	6.495E9	7.162E9
SA-1769 Peak Flux	5.524E9	5.931E9	6.250E9
WF-70 Peak Flux	6.019E9	6.159E9	6.905E9
WF-8/WF-18 Peak Flux	5.762E9	5.868E9	6.602E9
SA-1580 Peak Flux	5.523E9	5.313E9	6.232E9
Lower Plate Max Flux	6.169E9	6.303E9	7.162E9
Upper Plate Max Flux	6.173E9	6.495E9	7.084E9

Fluences for the vessel can also be extrapolated to longer time periods in order to estimate total fluences on the points of interest. This extrapolation is performed by assuming that the average fluence on the vessel for the extrapolated time is at equilibrium at the cycle 10 fluence. This assumption is acceptable provided that each subsequent cycle shows an equal or declining maximum fluence on the vessel surface. End of life fluences are determined by taking the cumulative fluence and then extrapolating forward. The cumulative fluence values for CR-3 through cycle 10 are shown in Table 2-2, along with the extrapolated EOL fluence at 15, 32, and 48 EFPY. The end of life (15, 32, or 48 EFPY) fluences are calculated using the following formula:

where $F(EOL)$ is the fluence estimate at the end of life (15, 32, or 48 EPFY), $F(EOC10)$ is the fluence at the end of cycle 10, ϕ_{10} is the flux for cycle 10, $t_{EOL}(s)$ is the total number of EPFS at the 15, 32, or 48 EPFY end of life (4.7335E6s, 1.0098E9 s, or 1.5147E9 s, respectively), and $t_{EOC10}(s)$ is the total number of EPFS accumulated through the end of cycle 10 (3.7462E8 s).

$$F(EOL) = F(EOC10) + (\phi_{10} * (t_{EOL}(s) - t_{EOC10}(s)))$$

Table 2-2. Cumulative Fluence Estimates

Cycle Length	Incremental Fluence (n/cm ²)			Cumulative Fluence (n/cm ²)					
	Cycles 7 & 8	Cycle 9	Cycle 10	EOC 6	EOC 10	Extrapolation Flux	15 EFPY	32 EFPY	48 EFPY
(EFPD)	1033.8	557.2	592.8						
(EFPS)	8.9320E7	4.8142E7	5.1218E7						
(EFPY)	2.830	1.526	1.623	5.876	11.8711		15	32	48
Flux Location	Incremental Fluence (n/cm ²)			Cumulative Fluence (n/cm ²)					
Inside Surface Max	5.514E17	3.127E17	3.668E17	2.0000E18	3.2309E18	7.5544E9	3.9768E18	8.0296E18	1.1844E19
SA-1769 Peak Fluence	4.934E17	2.856E17	3.201E17	1.7900E18	2.8891E18	6.5928E9	3.5401E18	7.0770E18	1.0406E19
WF-70 Peak Fluence	5.376E17	2.965E17	3.536E17	1.9200E18	3.1077E18	7.2832E9	3.8269E18	7.7342E18	1.1412E19
WF-8/WF-18 Peak Fluence	5.147E17	2.825E17	3.382E17	1.8400E18	2.9754E18	6.9645E9	3.6631E18	7.3994E18	1.0916E19
SA-1580 Peak Fluence	4.933E17	2.558E17	3.192E17	1.7200E18	2.7883E18	6.5744E9	3.4374E18	6.9644E18	1.0284E19
Lower Plate Max Fluence	5.510E17	3.034E17	3.668E17	1.9800E18	3.2012E18	7.5544E9	3.9472E18	7.9999E18	1.1814E19
Upper Plate Max Fluence	5.514E17	3.127E17	3.628E17	1.9300E18	3.1569E18	7.4727E9	3.8948E18	7.9037E18	1.1677E19

3.0 DOSIMETRY ACTIVITY

The ratio of the specified activities to the measured specific activities (C/M) is presented in Table 3-1 for cycles 9 and 10. In this table, the target averaged C/M represents the average of all the individual target dosimeters and the overall average is the average C/M for the entire capsule.

Table 3-1. C/M ratios

Cycle 9

Dos Type (b=bare)	Dosimeter	C	M	C/M	(C/M) AVG BY TYPE
Fe (b)	F	1.941E+00	1.897E+00	1.023E+00	1.021E+00
Fe (b)	G	1.941E+00	1.921E+00	1.010E+00	
Fe (b)	J	1.941E+00	1.930E+00	1.006E+00	
Fe(b)	AA	1.941E+00	1.911E+00	1.016E+00	
Fe	H	1.941E+00	1.897E+00	1.023E+00	
Fe	AB	1.941E+00	1.887E+00	1.029E+00	
Fe	AC	1.941E+00	1.844E+00	1.053E+00	
Fe	I	1.941E+00	1.927E+00	1.007E+00	1.061E+00
Ni	AM	3.618E+00	3.382E+00	1.070E+00	
Ni	AN	3.618E+00	3.371E+00	1.073E+00	
Ni	AO	3.618E+00	3.449E+00	1.049E+00	
Ni	AP	3.618E+00	3.444E+00	1.051E+00	9.995E-01
Cu	G	5.997E-03	6.034E-03	9.939E-01	
Cu	H	5.997E-03	5.975E-03	1.004E+00	
Cu	I	5.997E-03	5.983E-03	1.002E+00	
Cu	J	5.997E-03	6.008E-03	9.982E-01	1.034E+00
U-238	B4 U238	7.178E-03	6.945E-03	1.034E+00	
Nb	A	5.682E-01	4.852E-01	1.171E+00	1.189E+00
Nb	B	5.682E-01	4.824E-01	1.178E+00	
Nb	C	5.682E-01	4.617E-01	1.231E+00	
Nb	D	5.682E-01	4.834E-01	1.175E+00	
				OVERALL AVERAGE =	1.029E+00
					sans Nb & Np237

Cycle 10

DOSIM	note(s)	C	M	C/M	(C/M) AVG BY TYPE	
C		2.035E+00	1.737E+00	1.172E+00	1.168E+00	
F		2.035E+00	1.772E+00	1.148E+00		
G		2.035E+00	1.767E+00	1.152E+00		
B		2.035E+00	1.787E+00	1.139E+00		
D		2.035E+00	1.701E+00	1.196E+00		
E		2.035E+00	1.733E+00	1.174E+00		
H		2.035E+00	1.755E+00	1.160E+00		
I		2.035E+00	1.694E+00	1.201E+00		
O		3.259E+00	2.868E+00	1.136E+00		1.142E+00
P		3.259E+00	2.842E+00	1.147E+00		
A		6.627E-03	6.053E-03	1.095E+00	1.099E+00	
B		6.627E-03	6.008E-03	1.103E+00	1.012E+00	
U-1		7.910E-03	7.682E-03	1.030E+00		
U-2		7.910E-03	7.957E-03	9.941E-01		
NB-1		6.255E-01	5.742E-01	1.089E+00	1.088E+00	
NB-2		6.255E-01	5.756E-01	1.087E+00		
				OVERALL AVERAGE =	1.105E+00	
					sans Np237 & Nb	

4.0 REFERENCES

1. Worsham, J.R., et al., "Fluence and Uncertainty Methodologies," BAW-2241P-A, Revision 1, Framatome ANP, Lynchburg, Virginia, April 1999.
2. U.S. Nuclear Regulatory Commission Regulatory Guide 1.190, "Calculational and Dosimetry Methods for Determining Pressure Vessel Neutron Fluence," March 2001.
3. Rutherford, M. A., N. M. Hassan, et. al., Eds., "DORT, Two Dimensional Discrete Ordinates Transport Code," BWNT-TM-107, Framatome Technologies, Inc., Lynchburg, Virginia, May 1995.
4. Hassler, L. A., and N. M. Hassan, "SORREL, DOT Input Generation Code User's Manual," NPGD-TM-427, Revision 10, Framatome ANP, Lynchburg, Virginia, May 2001.
5. Ingersoll, D. T., et. al., "BUGLE-93, Production and Testing of the VITAMIN-B6 Fine Group and the BUGLE-93 Broad Group Neutron/photon Cross-Section Libraries Derived from ENDF/B-VI Nuclear Data," ORNL-DLC-175, Radiation Safety Information Computational Center, Oak Ridge National Laboratory, Oak Ridge, Tennessee, April 1994.
6. Hassler, L. A. and N. M. Hassan, "GIP User's Manual for B&W Version, Group Organized Cross Section Input Program," NPGD-TM-456, Revision 11, Framatome ANP, Lynchburg, Virginia, August 1994.
7. Worsham, J. R., "BUGLE-93 Response Functions," FTG Document Number 32-1232719-00, Revision 0, Framatome ANP, Lynchburg, Virginia, June 1995.
8. U.S. Nuclear Regulatory Commission, "Radiation Embrittlement of Reactor Vessel Materials," Regulatory Guide 1.99, Revision 2, May 1998.

- 9 Lowe, A. L., et. al., "Integrated Reactor Vessel Material Surveillance Program," BAW-1543A, Revision 2, Framatome ANP, Lynchburg, Virginia, May 1985.

APPENDIX A - METHODOLOGY

The primary tool used in the determination of the flux and fluence exposure to the surveillance capsule dosimeters is the two-dimensional discrete ordinates transport code DORT.³

The CR-3 PT analysis covers irradiation from cycle 7 through cycle 10, and includes capsules irradiated in cycles 9 and 10. The power distributions in the four irradiation cycles were symmetric both in θ and Z . That is, the axial power shape is roughly the same for any angle and, conversely, that the azimuthal power shape is the same for any height. This means that the neutron flux at some point (R, θ, Z) can be considered to be a separable function of (R, θ) and (R, Z) . Therefore, the cycle 7-10 irradiations can be modeled using the standard FANP synthesis procedures.¹

Figure A-1 depicts the analytical procedure that is used to determine the fluence accumulated over each irradiation period. As shown in the figure, the analysis is divided into seven tasks: (1) generation of the neutron source, (2) development of the DORT geometry models, (3) calculation of the macroscopic material cross sections, (4) synthesis of the results, and (5-7) estimation of the calculational bias, the calculational uncertainty, and the final fluence. Each of these tasks is discussed in greater detail in the following sections.

Generation of the Neutron Source

The time-averaged space and energy-dependent neutron sources for cycles 7-10 were calculated using the SORREL⁴ code. The effects of burnup on the spatial distribution of the neutron source were accounted for by calculating the cycle average fission spectrum for each fissile isotope on an assembly-by-assembly basis, and by determining the cycle-average specific neutron emission rate. This data was then used with the normalized time weighted average pin-

by-pin relative power density (RPD) distribution to determine the space and energy-dependent neutron source. The azimuthally averaged, time averaged axial power shape in the peripheral assemblies was used with the fission spectrum of the peripheral assemblies to determine the neutron source for the axial DORT run. These two neutron source distributions were input to DORT as indicated in Figure A-1. Three separate sources (7-8, 9 and 10) were developed in order to account for the two dosimetry capsules that were irradiated in cycles 9 and 10.

Development of the Geometrical Models

The system geometry models for the mid-plane (R, θ) DORT were developed using standard FANP interval size and configuration guidelines. The R0 model for the cycles 7-8, 9 and 10 analysis extended radially from the center of the core to the outer surface of the pressure vessel, and azimuthally from the major axis to 45°. The axial model extends from below the active core region to above the active core region. The geometrical models either met or exceeded all guidance criteria concerning interval size that are provided in Reg Guide 1.190.² In all cases, cold dimensions were used. The geometry models were input to the DORT code as indicated in Figure A-1. These models will be used in all subsequent pressure-temperature curve analyses that may be performed by FANP for CR-3.

Calculation of Macroscopic Material Cross Sections

In accordance with Reg Guide 1.190,² the BUGLE-93³ cross section library was used. The GIP code⁶ was used to calculate the macroscopic energy-dependent cross sections for all materials used in the analysis - from the core out through the cavity and into the concrete and from core plate to core plate. The ENDF/B-VI dosimeter reaction cross sections were used to

generate the response functions that were used to calculate the DORT-calculated "saturated" specific activities.

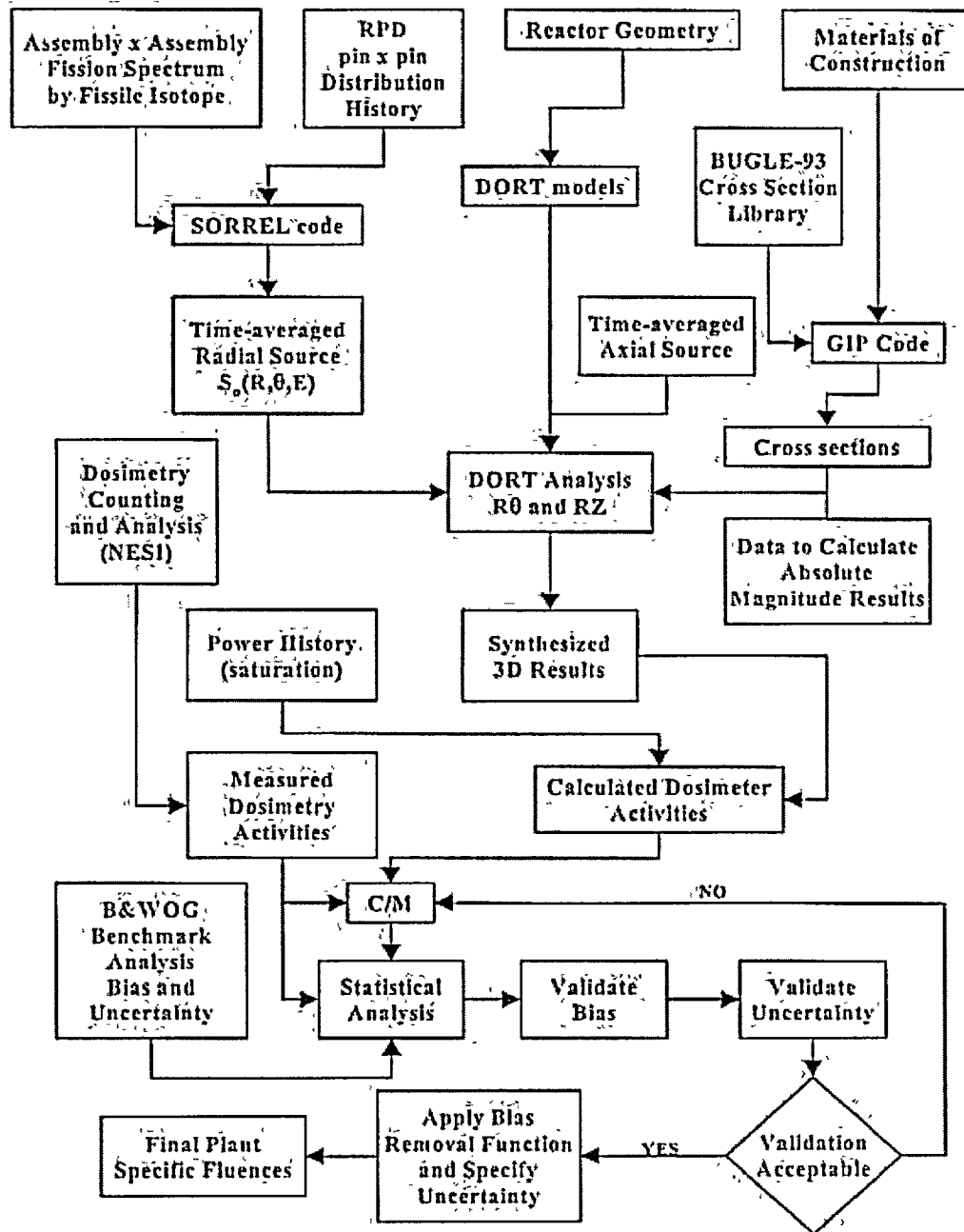


Figure A-1. Fluence Analysis Methodology for CR-3 PT Fluence Analysis

DORT Analyses

The cross sections, geometry, and appropriate source were combined to create a set of DORT models (R θ and RZ) for the cycles 7-8, 9, and 10 analyses. Each R θ DORT run utilized a cross section Legendre expansion of three (P_3), forty-eight directions (S_8), with the appropriate boundary conditions. The RZ models used a cross section Legendre expansion of three (P_3), forty-eight directions (S_8), with the appropriate boundary conditions. A theta-weighted flux extrapolation model was used, and all other requirements of Reg Guide 1.190² that relate to the various DORT parameters were either met or exceeded for all DORT runs.

Synthesized Three Dimensional Results

The DORT analyses produce two sets of two-dimensional flux distributions, one for a vertical cylinder and one for the radial plane for each set of dosimetry. The vertical cylinder, which will be referred to as the RZ plane, is defined as the plane bounded above and below the active core region and radially by the center of the core the outside surface of the reactor pressure vessel. The horizontal plane, referred to as the R θ plane, is defined as the plane bounded radially by the center of the core and the outside surface of the pressure vessel, and azimuthally by the major axis and the adjacent 45° radius. The vessel flux, however, varies significantly in all three cylindrical-coordinate directions (R, θ , Z). This means that if a point of interest is outside the boundaries of both the R-Z DORT and the R- θ DORT, the true flux cannot be determined from either DORT run. Under the assumption that the three-dimensional flux is a separable function,¹ both two-dimensional data sets were mathematically combined to estimate the flux at all three-dimensional points (R, θ , Z) of interest. The synthesis procedure outlined in Reg Guide 1.190² is identical to the basis used for the FANP flux-synthesis process.

Calculated Activities and Measured Activities

The calculated activities for each dosimeter type "d" for each irradiation period were determined using the following equation:

$$C_d = \sum_{g=1}^G \phi_g(\bar{r}_d) \times RF_g^d \times B_d \times NSF \quad (1)$$

where

C_d	...	calculated specific activity for dosimeter "d" in μCi of product isotope per gram of target isotope
$\phi_g(\bar{r}_d)$...	three dimensional flux for dosimeter "d" at position \bar{r}_d for energy group "g"
RF_g^d	...	dosimeter response function for dosimeter "d" and energy group "g"
B_d	...	bias correction factors for dosimeter "d"
NSF	...	non-saturation correction factor (NSF).

For this analysis, two separate sets of activities will be calculated, one for the dosimetry of cycle 9, and one for the dosimetry of cycle 10.

The bias correction factors (B_d) in the specific activity calculation above are listed in Table A-1.

Table A-0-1. Bias Correction Factors

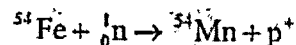
Dosimeter Type	Bias
Activation	Short Half Life
Fission	Photofission
	Impurities

A photofission factor was applied to correct for the fact that some of the ^{137}Cs atoms present in the dosimeter were produced by (γ, f) reactions and were not accounted for in DORT analysis. The short half life and impurity factors were insignificant and therefore were not applied.

C/M Ratios

The following explanations will define the meanings of the terms "measurements" (M) and "calculations" (C) as used in this analysis:

- **Measurements:** The meaning of the term "measurements" as used by FANP is the measurement of the physical quantity of the dosimeter (specific activity) that responded to the neutron fluence, not to the "measured fluence." For the example of an iron dosimeter, a reference to the measurements means the specific activity of ^{54}Mn in $\mu\text{Ci/g}$, which is the product isotope of the dosimeter reaction:



- **Calculations:** The calculational methodology produces two primary results – the calculated dosimeter activities and the neutron flux at all points of interest. The meaning of the term "calculations" as used by FANP is the calculated dosimeter activity. The calculated activities are determined in such a way that they are directly comparable to the measurement values, but without recourse to the measurements. That is, the calculated values are determined by the DORT calculation and are directly comparable to the measurement values. ENDF/B-VI based dosimeter reaction cross sections⁷ and response functions were used in

determining the calculated values for each individual dosimeter. In summary, it should be stressed that the calculation values in the FANP approach¹ are independent of the measurement values.

Uncertainty

The CR-3 Cycles 7-10 fluence predictions are based on the methodology described in the FANP "Fluence and Uncertainty Methodologies" topical report, BAW-2241P-A.¹ The time-averaged fluxes, and thereby the fluences throughout the reactor and vessel, are calculated with the DORT discrete ordinates computer code using three-dimensional synthesis methods. The basic theory for synthesis is described in Section 3.0 of the topical and the DORT three-dimensional synthesis results are the bases for the fluence predictions using the FANP "Semi-Analytical" (calculational) methodology.

The uncertainties in the CR-3 fluence values have been evaluated to ensure that the greater than 1.0 MeV calculated fluence values are accurate (with no discernible bias) and have a mean standard deviation that is consistent with the FANP benchmark database of uncertainties. Consistency between the fluence uncertainties in the updated calculations for CR-3 cycles 7-10 and those in the FANP benchmark database ensures that the vessel fluence predictions are consistent with the 10 CFR 50.61, Pressurized Thermal Shock (PTS) screening criteria and the Regulatory Guide 1.99¹ embrittlement evaluations.

The verification of the fluence uncertainty for the CR-3 reactor includes:

- estimating the uncertainties in the cycles 9 and 10 dosimetry measurements;

- estimating the uncertainties in the cycles 9 and 10 benchmark comparison of calculations to measurements,
- estimating the uncertainties in the cycles 7 through 10 pressure vessel fluence, and
- determining if the specific measurement and benchmark uncertainties for cycles 7-10 are consistent with the FANP database of generic uncertainties in the measurements and calculations.

The embrittlement evaluations in Regulatory Guide 1.99³ and those in 10 CFR 50.61 for the PTS screening criteria apply a margin term to the reference temperatures. The margin term includes the product of a confidence factor of 2.0 and the mean embrittlement standard deviation. The factor of 2.0 implies a very high level of confidence in the fluence uncertainty as well as the uncertainty in the other variables contributing to the embrittlement. The dosimeter measurements from the CR-3 cycles 9 and 10 analyses would not directly support this high level of confidence. However, the dosimeter measurement uncertainties are consistent with the FANP database. Therefore, the calculational uncertainties in the updated fluence predictions for CR-3 are supported by 728 additional dosimeter measurements and thirty-nine benchmark comparisons of calculations to measurements as shown in Appendix A of the topical.¹ The calculational uncertainties are also supported by the fluence sensitivity evaluation of the uncertainties in the physical and operational parameters, which are included in the vessel fluence uncertainty.¹ The dosimetry measurements and benchmarks, as well as the fluence sensitivity analyses in the topical are sufficient to support a 95 percent confidence level, with a confidence factor of ± 2.0 , in the fluence results from the "Semi-Analytical" methodology.

The FANP generic uncertainty in the dosimetry measurements has been determined to be unbiased and has an estimated standard deviation of 7.0 percent for the qualified set of dosimeters. The CR-3 cycles 9 and 10 dosimetry measurement uncertainties were evaluated to

determine if any biases were evident and to estimate the standard deviation. The dosimetry measurements were found to be appropriately calibrated to standards traceable to the National Institute of Standards and Technology and are thereby unbiased by definition. The mean measurement uncertainties associated with cycles 9 and 10 are as follows:

$$\sigma_{M(9)} = 6.24\%$$

$$\sigma_{M(10)} = 5.91\%$$

These values were determined from Equation 7.6 in the topical¹ and indicate that there is consistency with the FANP database. Consequently, when the FANP database is updated, the CR-3 cycles 9 and 10 dosimetry measurement uncertainties may be combined with the other 728 dosimeters. Since the cycles 9 and 10 measurements are consistent with the FANP database, it is estimated that the CR-3 dosimeter measurement uncertainty may be represented by the FANP database standard deviation of 7.0 percent. Based on the FANP database, there appears to be a 95 percent level of confidence that 95 percent of the CR-3 dosimetry measurements, for fluence reactions above 1.0 MeV, are within ± 14.2 percent of the true values.

The FANP generic uncertainty for benchmark comparisons of dosimetry calculations relative to the measurements indicates that any benchmark bias in the greater than 1.0 MeV results is too small to be uniquely identified. The estimated standard deviation between the calculations and measurements is 9.9 percent. This implies that the root mean square deviation between the FANP calculations of the CR-3 dosimetry and the measurements should be approximately 9.9 percent in general and bounded by ± 20.04 percent for a 95 percent confidence interval with thirty-nine independent benchmarks.

The weighted mean values of the ratio of calculated dosimeter activities to measurements (C/M) for cycles 9 and 10 have been statistically evaluated using Equation 7.15 from the topical.¹

The standard deviation in the benchmark comparisons is as follows:

$$\sigma_{\frac{C}{M}}^{(9)} = 2.86\%$$

$$\sigma_{\frac{C}{M}}^{(10)} = 10.05\%$$

This standard deviation indicates that the benchmark comparisons are consistent with the FANP database. Consequently, when the FANP database is updated, the cycles 9 and 10 benchmark uncertainties may be included with the other thirty-nine benchmark uncertainties in the topical.¹ The consistency between the cycles 9 and 10 benchmark uncertainties and those in the FANP database indicates that the CR-3 fluence calculations for cycles 7-10 have no discernible bias in the greater than 1.0 MeV fluence values. In addition, the consistency indicates that the fluence values can be represented by the FANP reference set which includes a calculational standard deviation of 7.0 percent at dosimetry locations. That is:

Table A-2. Calculational Fluence Uncertainties

Type of Calculation	Uncertainty (%)	
	Standard Deviation (σ)	95% / 95% Confidence ($\approx \pm 2\sigma$)
Capsule	7.0	14.2
Pressure Vessel (maximum location)	10.0	20.0
Pressure Vessel (extrapolation)	11.4	22.8